

Determination of the mobility edge in the Anderson model of localization in three dimensions by multifractal analysis

H. Grussbach

Institut für Physikalische Chemie, Johannes-Gutenberg-Universität, Jakob-Welder-Weg 11, D-55099 Mainz, Federal Republic of Germany

M. Schreiber

Institut für Physik, Technische Universität, D-09107 Chemnitz, Federal Republic of Germany

(Received 11 October 1994)

We study the Anderson model of localization in three dimensions with different probability distributions for the site energies. Using the Lanczos algorithm we calculate eigenvectors for different model parameters like disorder and energy. From these we derive the singularity spectrum typically used for the characterization of multifractal objects. We demonstrate that the singularity spectrum at the critical disorder, which determines the mobility edge at the band center, is independent of the employed probability distribution. Assuming that this singularity spectrum is universal for the metal-insulator transition regardless of specific parameters of the model we establish a straightforward method to distinguish localized and extended states. In this way we obtain the entire mobility-edge trajectory separating regions of extended states from regions of localized states in the energy-disorder phase diagram. The good agreement with results from transfer-matrix calculations for all probability distributions used corroborates the applicability of our criterion.

The theoretical investigation of the localization problem in disordered systems is of central importance for a variety of different phenomena like transport properties of glassy or amorphous systems. Particularly interesting are systems that feature a metal-insulator transition (MIT). Due to this transition, the electronic wave functions show a characteristic change from localized to extended behavior. This corresponds to a change from states that do not enable transport in the limit of vanishing temperature to states that do, thus distinguishing the insulating and metallic character.¹

In the localized regime the spatial behavior of the wave functions is usually described by an exponential decay length reflecting the spatial extent of the wave function. This method, however, suffers from large fluctuations of the amplitude of the wave function especially for states close to the MIT. Approaching the MIT from the localized regime the localization length diverges. Close to the MIT the localization length is already much larger than the numerically accessible system size so that there can be no direct reflection of the localization in the calculated eigenstate. Rather the computation yields the mentioned fluctuations only.

Approaching the MIT from the extended regime the behavior is analogous. Here the respective characteristic length is the correlation length which diverges approaching the MIT. Numerically, the correlation length is not directly accessible due to fluctuations of the wave function. In this paper we will exploit exactly these fluctuations for the characterization of the states, allowing a determination of the MIT.

Exactly at the MIT where there is no characteristic length scale the suggestion that the eigenstates show fractal characteristics² was confirmed by several numerical investigations (for an overview see Ref. 3). However, it became clear that the characterization of eigenstates at the transition requires the more general concept of multifractality.⁴ This implies that different parts of the eigenstate scale with dif-

ferent exponents thus extending the simple fractal picture which comprised only one scaling exponent.

The standard way to characterize multifractals which have appeared in many different parts of physics, for example in turbulence, diffusion limited aggregates (DLA), viscous fingering, etc.⁵ is the singularity spectrum or, equivalently, the continuous set of generalized dimensions. It was noticed that for the Anderson model of localization in three dimensions³ (3D) as well as in 2D with magnetic field^{6,7} the MIT corresponds to a characteristic singularity spectrum. This result led to the expectation that the transport properties can be related quantitatively to the singularity spectrum. We have shown recently,⁸ that the system size dependence of the singularity spectrum can be used to distinguish localized and extended states in 3D at the band center. We have also been able⁹ to determine the MIT at the band edge from the singularity spectrum.

In this paper we show that the shape of the singularity spectrum at the MIT does not depend on the probability distribution used for the site energies in the Anderson Hamiltonian. This suggests that the critical singularity spectrum is universal and thus not dependent on energy or disorder. We test this assumption by using the critical singularity spectrum for the distinction of localized and extended states in the entire energy-disorder phase diagram. The resulting mobility edge trajectory is shown to agree with results obtained previously by another method.

To investigate the Anderson model of localization we use the standard Hamiltonian $H = \sum_i |i\rangle \varepsilon_i \langle i| + \sum_{i,j} |i\rangle \langle j|$. The first term describes the disorder by random site energies ε_i usually taken from a box distribution of width W on a regular cubic lattice in 3D. In addition, we study the Gaussian and the binary (or dichotomic) distribution. In analogy to the box distribution we define the disorder parameter $W = \sigma/\sqrt{12}$ in

terms of the second moment σ in all cases. Furthermore we choose the average (first moment) $\langle \varepsilon \rangle = 0$ without loss of generality. The investigation of the binary distribution is restricted to the symmetric case, i.e., $P(\varepsilon) = \frac{1}{2}\delta(\varepsilon - W/\sqrt{3}) + \frac{1}{2}\delta(\varepsilon + W/\sqrt{3})$. The second part of the Hamiltonian consists of constant transfer elements which are taken between nearest neighbors only. We set $V = 1$ fixing the energy scale.

Applying the transfer-matrix method (TMM) to the Anderson Hamiltonian the exponential decay of electronic states in quasi-1D systems can be determined. Its dependence on the (lateral) system size yields conclusions about the localization and the correlation length. Extensive computations were necessary to derive the mobility edge for box and Gaussian distribution.¹⁰⁻¹² In both cases the maximal value of the critical disorder occurs in the center of the band ($E = 0$), it is $W_c = 16.5$ for the box and $W_c = 20.9$ for the Gaussian distribution.

The binary distribution yields increasing critical disorders for increasing energy. This can be traced back to the specific shape of the density of states in this model¹⁰ which features two distinct subbands around $E = \pm W/\sqrt{3}$ for large disorder corresponding to two separate percolating networks of sites with $\varepsilon_i > 0$ and $\varepsilon_i < 0$, respectively. Here, only a few TMM results are available,¹⁰ in particular $W_c(E = 0) = 9.1$.

We employ the Lanczos algorithm¹³ for the direct computation of the eigenstates. This algorithm is especially suited for large sparse matrices as described by the Hamiltonian above. Indeed it was possible to treat samples with more than 250 000 sites in 3D in the band center.⁸ At the band edges the algorithm allows us to investigate even larger systems. To facilitate vectorization on supercomputers we have used helical boundary conditions instead of the more common periodic ones. Furthermore it should be noted, that the algorithm enables the simultaneous computation of several eigenstates in a certain energy range allowing us to average the singularity spectra of several eigenstates without repeating the algorithm.

For the computation of the singularity spectrum we use the standard box-counting method.¹⁴⁻¹⁷ First we divide the system with N^3 sites into $N_L = N^3/L^3$ boxes of linear size L . The probability to find an electron in such a box is given by $\mu_k(L) = \sum_{n=1}^{L^3} |e_{in}|^2$ for $k = 1, \dots, N_L$ where e_{in} denotes the amplitude of an eigenstate with energy E_i at site n . The normalized q th moment of this probability $\mu_k(q, L) = \mu_k^q(L) / \sum_{k'=1}^{N_L} \mu_{k'}^q(L)$ constitutes a measure. From this one obtains the Lipschitz-Hölder exponent or singularity strength

$$\alpha(q) = \lim_{\delta \rightarrow 0} \sum_{k=1}^{N_L} \mu_k(q, L) \ln \mu_k(1, L) / \ln \delta \quad (1a)$$

and the corresponding fractal dimension

$$f(q) = \lim_{\delta \rightarrow 0} \sum_{k=1}^{N_L} \mu_k(q, L) \ln \mu_k(q, L) / \ln \delta, \quad (1b)$$

which yield the characteristic singularity spectrum $f(\alpha)$ in a parametric representation. Here, $\delta = L/N$ denotes the ratio of the box size and the system size. From Eq. (1) one can obtain

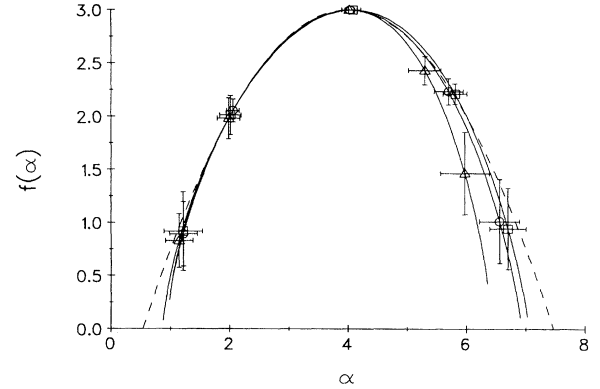


FIG. 1. Singularity spectrum at $E = 0$ and W_c for box (\circ), Gaussian (\square), and binary (\triangle) probability distribution. Integer values of the implicit parameters q are marked by symbols for $|q| \leq 2$. Error bars are due to the statistical error from averaging over disorder realizations and energy range. The dashed line shows the analytical result of Wegner (Ref. 18).

the generalized dimensions $D(q) = \{f[\alpha(q)] - q\alpha(q)\} / (1 - q)$. As pointed out by different authors (e.g., Ref. 17) the main problem of this approach is the proposed linearity of $\sum \mu \ln \mu$ versus $\ln \delta$. At least at and close to the MIT this is fulfilled.⁸ It is clear, however, that far away from the MIT the linearity is destroyed. This will occur whenever the characteristic length scale becomes smaller than the system size. For disorders close to but not exactly at the mobility edge in 3D the singularity spectrum changes characteristically with the system size.⁸ Only exactly at the MIT the singularity spectrum remains unchanged. Correspondingly in the limit of infinite system size multifractality is expected to hold only exactly at the MIT, all other states are either localized or extended.

We have calculated the singularity spectra for systems with $20^3 = 8000$ sites for several disorders W and energies E . All eigenstates in a given energy range of $\Delta E = 0.01$ at a specific disorder W were determined in one run of the Lanczos algorithm. For each eigenstate we derive the values of $\alpha(q)$ and $f(q)$ according to Eq. (1) and average over this energy range and additionally over five different realizations of the disorder (i.e., five different Lanczos runs). In that way we average typically over about 20 different states (depending on the density of states) for one parameter combination. At the band edge the energy interval was increased up to $\Delta E = 0.05$ because of the low density of states there. The calculations could be done on a PC in a few hours.

In Fig. 1 we present the results at the MIT for $E = 0$ for all probability distributions used in this study. Here we took for granted the critical disorder values from the TMM mentioned above. The discussed criterion that $f(\alpha)$ does not change with the system size only at the MIT (Ref. 8) yields critical disorders which are in agreement within the numerical accuracy, which is, however, not very high for this criterion.

The coincidence of the three curves in Fig. 1 is remarkable. It demonstrates that the singularity spectrum takes a specific shape at the MIT, independent of the employed probability distribution. We note that this critical spectrum agrees with the analytical result derived in the nonlinear σ model performing the ε expansion to first order¹⁸ which is also

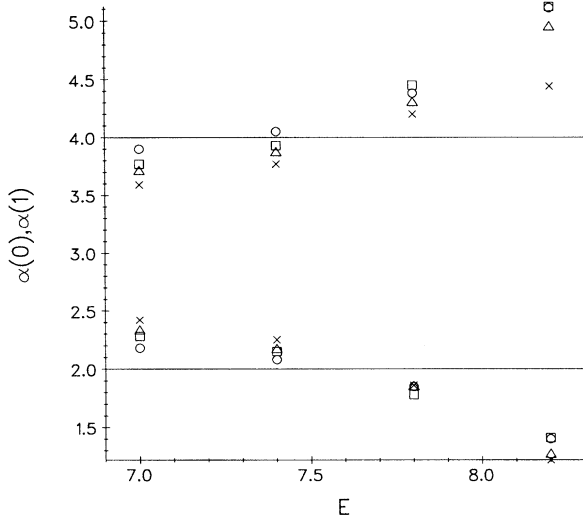


FIG. 2. Behavior of $\alpha(0)$ and $\alpha(1)$ at $W=12$ with changing E and N for the box distribution. Different symbols denote different system sizes according to $N^3=20^3$ (\circ), 30^3 (\square), 40^3 (\triangle), and 60^3 (\times).

shown in Fig. 1. We propose that this specific shape is independent of energy and disorder, too.

Before we proceed to corroborate this claim with our results, it is useful to recall a few general features of the singularity spectrum which can be observed in Fig. 1, too. The singularity spectrum is bound from below by zero, it is convex, its maximum is obtained for $q=0$ and reflects the dimension of the support of the measure which in our case is 3, i.e., $f[\alpha(0)]=D(0)=3$. This is the similarity dimension. Important is also the information or entropy dimension reached for $q=1$. At this point the relation $f[\alpha(1)]=\alpha(1)=D(1)$ is fulfilled. One can show that in the limit of infinite system size the entire measure is concen-

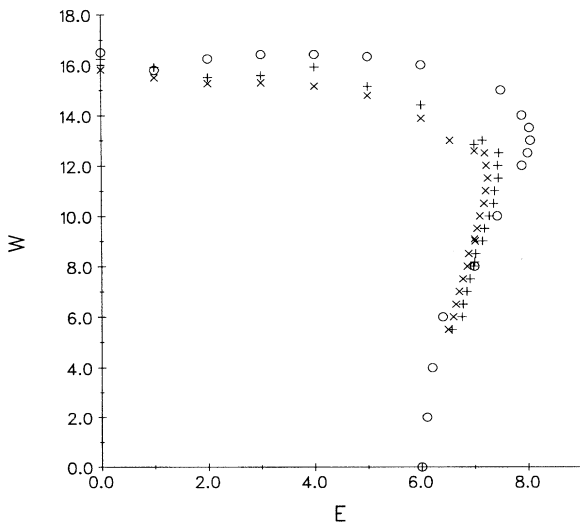


FIG. 3. The mobility edge trajectory in 3D as calculated by the TMM (\circ) (from Ref. 11) and the multifractal analysis via $\alpha(0)$ (\times) and $\alpha(1)$ ($+$) for the box distribution.

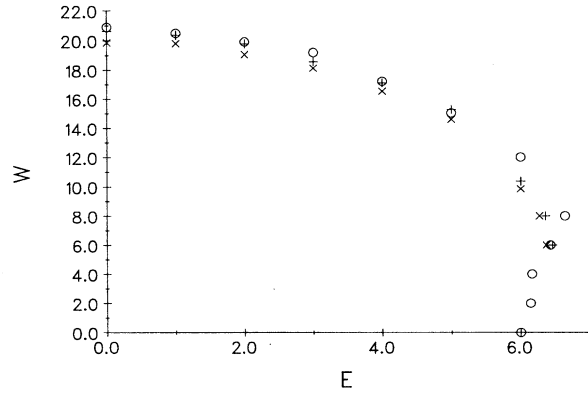


FIG. 4. Same as Fig. 3 but for the Gaussian distribution, TMM data from Ref. 11.

trated into a fractal set with this dimension.

We concentrate the subsequent analysis to these two points of the singularity spectrum ($q=0$ and $q=1$) not only because they reflect significant dimensions but also because the evaluation of Eq. (1) is numerically more accurate for small values of $|q|$. Specifically we obtain at the MIT the critical values of $\alpha_c(0)=4$ and $\alpha_c(1)=2$ from Fig. 1 approximately and from the analytical formula exactly.¹⁸ These values are now employed to distinguish localized and extended wave functions for various parameter combinations (E, W). As an example we display in Fig. 2 the dependence of $\alpha(0)$ and $\alpha(1)$ on E for fixed disorder $W=12$ for the box distribution. We expect⁸ $\alpha(0) > \alpha_c(0)$ and $\alpha(1) < \alpha_c(1)$ for localized states but $\alpha(0) < \alpha_c(0)$ and $\alpha(1) > \alpha_c(1)$ for extended states. Accordingly we derive $E_c \approx 7.5$ by extrapolating the $\alpha(0)$ data for $N=20$ and $E_c \approx 7.6$ from the respective $\alpha(1)$ values, in good agreement with the TMM results indicated in Fig. 3. We note that the data for larger N will yield slightly larger E_c values in even better agreement with the TMM results.

This procedure is now performed for various E and W , yielding $W_c(E)$ or $E_c(W)$, respectively, which are shown in Figs. 3–5. The agreement with the TMM is very good for the Gaussian disorder whereas for the box distribution the coincidence is not so good for large W at the band edge. However, the reentrant behavior of the mobility edge (the change from localized to extended and back to localized behavior upon increasing disorder for certain fixed energies) is clearly reproduced.

In order to check for the size dependence we have also calculated systems with $N^3=30^3=27\,000$, $N^3=40^3=64\,000$, and $N^3=60^3=216\,000$ sites for $W=12$ (cf. Fig. 2) and other parameters, but found no significant change in the reentrant behavior of the mobility edge. However, the character of the eigenstates in that region changes very fast with E which renders the analysis delicate. For the system size $N^3=20^3$ and low disorder $W \leq 5$ even the state at highest energy remains extended, only for larger systems localized states appear.

For the binary distribution in the center of the band the critical disorder $W_c=9.1$ (Ref. 10) is also correctly reproduced. For higher energies the value of the critical disorder increases as expected. At $E=6$ a second mobility edge ap-

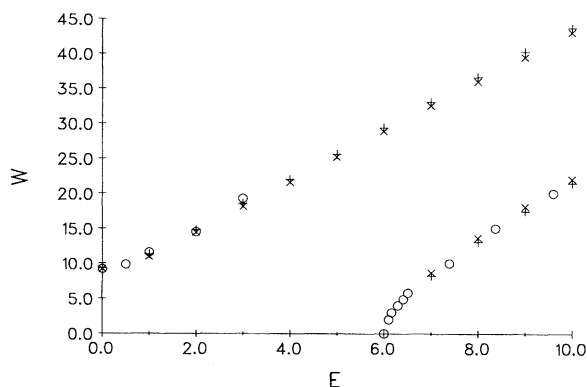


FIG. 5. Same as Fig. 3 but for the binary distribution, TMM data from Ref. 10.

pears, its starting point at $E=6$, $W=0$ corresponds to the (extended) Bloch state with highest energy in an ordered 3D system. For nonzero disorder localized states occur at this band edge. Together with the other edge (starting at $E=0$, $W_c=9.1$) in Fig. 5 the band of extended states around $E=W/\sqrt{3}$ can be seen clearly. Arising from the percolating network formed by the sites with $\varepsilon_i=W/\sqrt{3}$, the width of this band is consistent with the average number of three nearest neighbors in this network. Figure 5 demonstrates that in the binary case these extended states exist for arbitrary large disorder.

Finally we would like to comment on the connection between the multifractal behavior of the wave function and the critical exponent. It has been shown in 2D (Ref. 19) that from the correlation dimension $D(2)=2\alpha(2)-f[\alpha(2)]$ one can obtain a lower bound for the critical exponent ν as $\nu \geq 2/D(2)$. We have calculated $D(2)$ for all parameter combinations and probability distributions used. By using the W_c values from the analysis of $\alpha(0)$, i.e., the respective data

(\times) from Figs. 3–5, for energies in the range $0 \leq E \leq 6$ we find that $\nu=1.32 \pm 0.02$, 1.31 ± 0.02 , and 1.25 ± 0.04 for box, Gaussian, and binary distribution. Using respective W_c values from the $\alpha(1)$ analysis, i.e., the respective data (+) from Figs. 3–5, we determine $\nu \geq 1.37 \pm 0.01$, 1.37 ± 0.02 , and 1.33 ± 0.01 . The statistical errors arise from averaging $D(2)$ in the range. These values are in very good agreement with the value $\nu=1.35$ found recently.²⁰ It remains a puzzle however, why the lower bound is reached almost exactly. For energies close to the band edge the value of $D(2)$ fluctuates very much due to the very sensitive dependence of the critical disorder on energy but obeys $1.45 \leq D(2) \leq 1.8$ in all parameter combinations used.

In summary we have shown, that the very fluctuations of the eigenstates which hitherto were considered a nuisance in the numerical investigations can be profitably exploited by means of a multifractal analysis. The resulting singularity spectrum can be used to distinguish localized and extended states thus enabling us to calculate the mobility edge for systems with different probability distributions for the random site energies. The results were compared whenever possible with TMM calculations and gave reasonable agreement. Already for very small systems the accuracy of the method is sufficient to obtain a good qualitative description of the mobility edge. If one increases the system size one can hope for an even more accurate picture. We note that the system size for the mentioned TMM calculations was three orders of magnitude larger.

The present investigation was concentrated on two points $\alpha(0)$ and $\alpha(1)$ of the singularity spectrum. but in principle one can apply the method to any other point $\alpha(q)$ or $f(q)$. An interesting open question is whether finite size scaling of the $\alpha(q)$ or $f(q)$ data for different system sizes is feasible thus enabling us to determine a critical exponent from the spatial fluctuations of the eigenstate in a similar way as it was possible from the energetic fluctuations of the eigenvalue spectrum.²⁰

- ¹For an overview, see *Anderson Transition and Mesoscopic Fluctuations*, edited by B. Kramer and G. Schön [Physica **A167** (1990)].
- ²H. Aoki, J. Phys. C **16**, L205 (1983).
- ³M. Schreiber and H. Grussbach, Mod. Phys. Lett. **B6**, 851 (1992).
- ⁴M. Schreiber and H. Grussbach, Phys. Rev. Lett. **67**, 607 (1991).
- ⁵J. Feder, *Fractals* (Plenum, New York, 1988).
- ⁶W. Pook and M. Janssen, Z. Phys. B **82**, 295 (1991).
- ⁷B. Huckestein and L. Schweitzer, in *High Magnetic Fields in Semiconductor Physics III*, edited by G. Landwehr, Springer Series in Solid State Sciences Vol. 101 (Springer, Berlin, 1992), p. 84.
- ⁸H. Grussbach and M. Schreiber, Chem. Phys. **178**, 733 (1993).
- ⁹M. Schreiber and H. Grussbach, J. Fractals **1**, 1037 (1993).
- ¹⁰M. Ottomeier, Diploma thesis, Universität Dortmund, 1991.
- ¹¹B. Bulka, M. Schreiber, and B. Kramer, Z. Phys. B **66**, 21 (1987).
- ¹²B. Kramer, K. Broderix, A. MacKinnon, and M. Schreiber, Physica **A167**, 163 (1990).
- ¹³J. K. Cullum and R. A. Willoughby, *Lanczos Algorithms for Large Symmetric Eigenvalues Computations*, Vol. 1, Theory (Birkhäuser, Basel, 1985).
- ¹⁴A. B. Chhabra and R. V. Jensen, Phys. Rev. Lett. **62**, 1327 (1989).
- ¹⁵H. G. E. Hentschel and I. Procaccia, Physica **D8**, 435 (1983).
- ¹⁶T. C. Halsey, M. H. Jensen, L. P. Kadanoff, I. Procaccia, and B. I. Shraiman, Phys. Rev. A **33**, 1141 (1986).
- ¹⁷C. J. G. Evertsz and B. B. Mandelbrot, in *Chaos and Fractals* edited by H. O. Peitgen, H. Jürgens, and D. Saupe (Springer, Heidelberg, 1992), Appendix B.
- ¹⁸F. Wegner, Nucl. Phys. **B316**, 663 (1989).
- ¹⁹B. Kramer, Phys. Rev. B **47**, 9888 (1993); M. Janssen, Int. J. Mod. Phys. B **8**, 943 (1994).
- ²⁰E. Hofstetter and M. Schreiber, Phys. Rev. B **49**, 14 726 (1994).